Molecular Plant Pathology

MOLECULAR PLANT PATHOLOGY (2012) **13**(6), 531–545 DOI: 10.1111/J.1364-3703.2011.00770.X

Transcriptome analysis of *Stagonospora nodorum*: gene models, effectors, metabolism and pantothenate dispensability

SIMON V. S. IPCHO[1], JAMES K. HANE[1,2], EVA A. ANTONI[1], DAG AHREN[3], BERNARD HENRISSAT[4], TIMOTHY L. FRIESEN[5], PETER S. SOLOMON[6] AND RICHARD P. OLIVER[7,*]

[1]*Murdoch University, Heath Science, Murdoch, WA 6150, Australia*
[2]*Division of Plant Industry, CSIRO Centre for Environment and Life Sciences, Floreat, WA 6014, Australia*
[3]*Microbial Ecology, Lund University, Box 118, SE-22100 Lund, Sweden*
[4]*CNRS & Université de la Mediterranée, 13288 Marseille Cedex 9, France*
[5]*USDA-ARS Cereal Crops Research Unit, Northern Crop Science Laboratory, 1307 18th Street North, Fargo, ND 58105, USA*
[6]*Research School of Biology, The Australian National University, Canberra, ACT 0200, Australia*
[7]*Australian Centre for Necrotrophic Fungal Pathology, Department of Environment and Agriculture, Curtin University, Bentley, WA 6845, Australia*

SUMMARY

The wheat pathogen *Stagonospora nodorum*, causal organism of the wheat disease Stagonospora nodorum blotch, has emerged as a model for the Dothideomycetes, a large fungal taxon that includes many important plant pathogens. The initial annotation of the genome assembly included 16 586 nuclear gene models. These gene models were used to design a microarray that has been interrogated with labelled transcripts from six cDNA samples: four from infected wheat plants at time points spanning early infection to sporulation, and two time points taken from growth in artificial media. Positive signals of expression were obtained for 12 281 genes. This represents strong corroborative evidence of the validity of these gene models. Significantly differential expression between the various time points was observed. When infected samples were compared with axenic cultures, 2882 genes were expressed at a higher level *in planta* and 3630 were expressed more highly *in vitro*. Similar numbers were differentially expressed between different developmental stages. The earliest time points *in planta* were particularly enriched in differentially expressed genes. A disproportionate number of the early expressed gene products were predicted to be secreted, but otherwise had no obvious sequence homology to functionally characterized genes. These genes are candidate necrotrophic effectors. We have focused attention on genes for carbohydrate metabolism and the specific biosynthetic pathways active during growth *in planta*. The analysis points to a very dynamic adjustment of metabolism during infection. Functional analysis of a gene in the coenzyme A biosynthetic pathway showed that the enzyme was dispensable for growth, indicating that a precursor is supplied by the plant.

*Correspondence: Email: richard.oliver@curtin.edu.au

INTRODUCTION

The biological properties of an organism are determined by the expression of its complement of genes and the interaction with the environment. As genome sequences of an increasing number of fungal plant pathogens are being established, it is now possible to determine comprehensively not only which genes are present, but also which genes are expressed during different phases of infection. Such knowledge is the basis on which to elucidate the molecular details of pathogenicity and to deduce novel methods of control.

Transcriptomics is a powerful tool for the functional characterization of genes. A whole-genome assembly permits the design of microarrays that include elements reporting the expression of all annotated genes. Although many fungal microarray studies have been published (Breakspear and Momany, 2007), only a handful refer to sequenced pathogens (Tan *et al*., 2009). These have so far been limited to the Sordariomycete, hemibiotrophic rice and wheat pathogens *Magnaporthe grisea* (Dean *et al*., 2005; Donofrio *et al*., 2006) and *Fusarium graminearum* (Guldener *et al*., 2006; Stephens *et al*., 2008) and the Basidiomycete, biotrophic maize pathogen *Ustilago maydis* (Brefort *et al*., 2009; Eichhorn *et al*., 2006; Kamper *et al*., 2006; Tan *et al*., 2009).

Stagonospora (teleomorph: *Phaeosphaeria*, syn. *Septoria*) *nodorum* is a major necrotrophic pathogen of wheat causing the disease Stagonospora nodorum (syn. glume) blotch (Solomon *et al*., 2006b), which is responsible for large yield losses in parts of Australia (Murray and Brennan, 2009), the Americas and Asia. It is a member of the class Dothideomycetes, which includes such economically important and scientifically interesting pathogenic genera as *Cochliobolus*, *Leptosphaeria*, *Alternaria*, *Venturia*, *Mycosphaerella*, *Pyrenophora* and *Passalora* (Hane *et al*., 2007, 2011; Schoch *et al*., 2006, 2009). The genome assembly of *S. nodorum* (Hane *et al*., 2007) was the first Dothideomycete to be published. More recently, the barley net-blotch pathogen *Pyrenophora teres*, the wheat pathogen *Mycosphaerella graminicola* and the canola pathogen *Leptosphaeria maculans* have been analysed (Ellwood *et al*., 2010; Goodwin *et al*., 2011; Rouxel *et al*., 2011).

Automatic gene annotation of genome assemblies is an imprecise process. Preliminary gene calling on the *S. nodorum* genome defined 16 586 nuclear genes, significantly higher than the rather consistent *c*. 12 000 found in a range of more intensively studied filamentous fungi (Hane *et al*., 2007). A more stringent gene-calling procedure, supported by expressed sequence tag (EST) sequencing, predicted 10 762 nuclear genes. More recently, proteogenomics has been used to validate 2134 genes (Bringans *et al*., 2009). There remains a large degree of uncertainty in the reliability of *in silico*-predicted gene models, and comprehensive microarrays are an efficient method of gene validation.

Although *S. nodorum* is an archetypal necrotrophic fungus (Oliver and Ipcho, 2004), its recently revealed properties belie the crude reputation of this group. A series of studies has shown that the interaction between wheat and *S. nodorum* is governed, to a large degree, by the interplay of several specific necrotrophic effectors (previously called host-specific toxins) and their matching host recognition genes (Faris *et al*., 2010; Friesen *et al*., 2002, 2003, 2006, 2007, 2008; Liu *et al*., 2006, 2009; Meinhardt *et al*., 2002; Oliver and Solomon, 2010). One result of these studies is that the pathogen population can be divided into races that express different combinations of necrotrophic effectors. In this study, we used an isolate believed to produce no necrotrophic effectors, Sn79-1087 (Friesen *et al*., 2006), so as to be in a position to identify further effector candidates and, more directly, as a control for background signal elimination.

We have generated a comprehensive gene-based microarray of the genome and interrogated it with RNA from infected plant material sampled at four time points and from axenic material at two. The dataset represents an important resource to unravel specific and general mechanisms of pathogenicity in Dothideomycetes, in other cereal pathogens and in other necrotrophic fungi.

Only limited information on the biochemical basis of infection in necrotrophic pathogens is available. We have used the transcriptomic data to infer the activity of selected biochemical pathways. This analysis has focused on carbohydrate metabolism and the specific biosynthetic pathways either required or optional for growth in plants. The analysis points to a very dynamic adjustment of metabolism during infection. Functional analysis of a gene in the pantothenate to coenzyme A (CoA) biosynthetic pathway was undertaken because the pathway genes were surprisingly expressed at a lower level during infection. We have shown that the enzyme is dispensable for growth, indicating that a precursor is supplied by the plant.

RESULTS AND DISCUSSION

The *S. nodorum* SN15 genome sequence (Hane *et al*., 2007) was used to design a custom whole-genome microarray. Probe sets (referred to henceforth as genes) were designed for 16 085 of the predicted genes. Mitochondrial and transposon genes were omitted. Samples from different stages of the fungal life cycle (Solomon *et al*., 2006d) (Fig. 1) were collected and the transcriptome was analysed using the microarray. At 3 days post-inoculation (dpi), the fungus had infiltrated the leaf and caused necrosis at the site of infection. Infection samples from earlier time points were not collected because of insufficient fungal biomass. Leaf samples at 5 dpi *in planta* showed progression of necrosis, but no asexually differentiated structures could be observed. Pycnidiation was first observed on necrotic tissue at 7 dpi and was widespread by 10 dpi. Axenic (*in vitro*) cultures at 4 and 16 dpi were collected to analyse vegetative and sporulating mycelium. The avirulent strain Sn79-1087 was also grown for 4 days on minimal medium for comparison with the virulent strain SN15.

The quality and reliability of the data were analysed by comparing quantitative reverse transcription-polymerase chain reaction (qRT-PCR) results with array data (Figs S1 and S2, see Supporting Information). In all cases, data were consistent. Reciprocal inconsistencies between probes for a single gene have been associated with alternative splicing (Jung *et al*., 2009). No obvious alternative splicing candidates were obtained in this study (data not shown).

Principal component analysis

Principal component analysis was used to assess and visualize the data (Fig. 2). There was clear differentiation within and between *in planta* and *in vitro* samples. The early (3 and 5 dpi) *in planta*

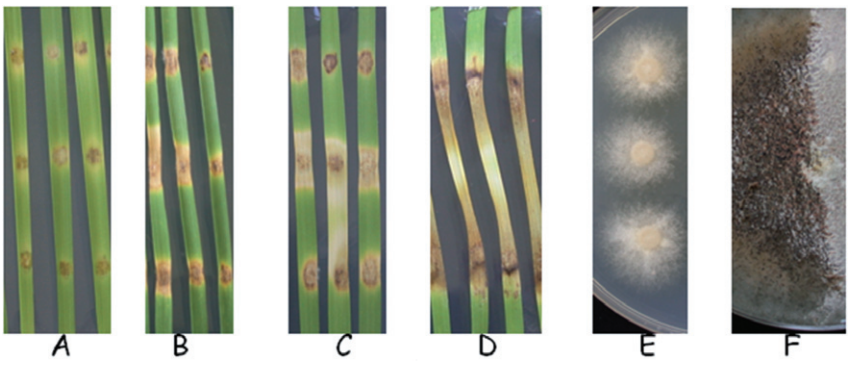

Fig. 1 Leaf infections and axenic cultures used for RNA extraction. (A–D) Infected leaf samples from 3, 5, 7 and 10 days post-inoculation (dpi), corresponding to early infection, vegetative state, sporulation and late infection stages, respectively. (E, F) Samples in minimal medium for 4 and 16 days, corresponding to vegetative growth and sporulation, respectively.

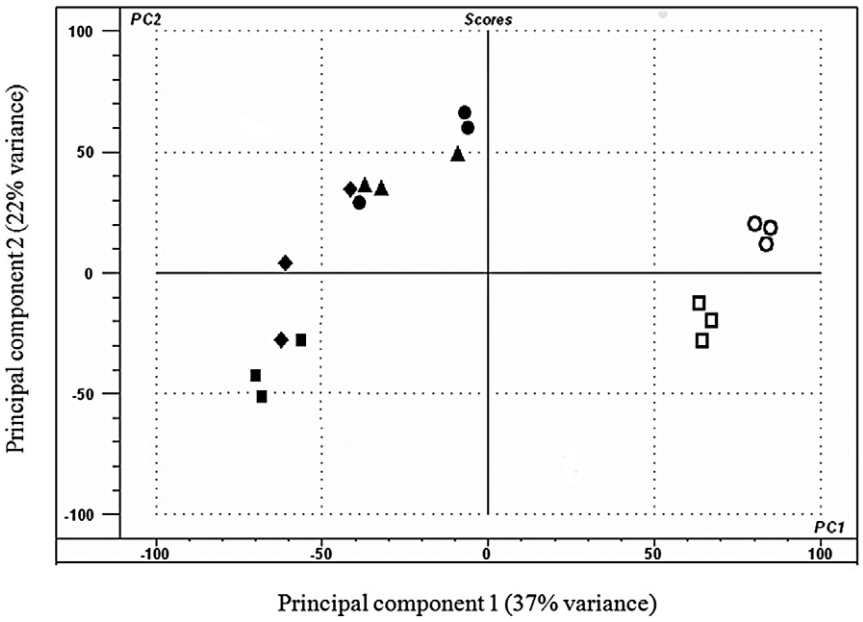

Fig. 2 Principal component analysis of the expression profile from 18 sample datasets using The Unscrambler® software (CAMO, Oslo, Norway). The samples used consisted of materials in triplicate from detached leaf assays infected with *Stagonospora nodorum* SN15 [3 dpi *in planta* (■), 5 dpi *in planta* (◆), 7 dpi *in planta* (●) and 10 dpi *in planta* (▲)] and axenically grown SN15 [4 dpi *in vitro* (□) and 16 dpi *in vitro* (○)]. Principal component 1 (PC1) accounted for 37% of the variation and principal component 2 (PC2) described 22% of the variation. PC1 mainly differentiates samples according to the growth medium, whereas PC2 mainly differentiates samples according to their developmental stage. dpi, days post-inoculation.

samples showed a moderate degree of overlap, and the 7- and 10-dpi samples were not significantly differentiated. PC1 describes 37% of the variance and clearly differentiates the *in vitro* samples from the *in planta* samples. PC2, accounting for 22% of the variance, differentiates the samples mainly according to their developmental stages. On the basis of these results, the 7- and 10-dpi datasets were merged and are referred to as 'late *in planta*'.

The clear separation of many clusters illustrates that very distinct sets of genes are transcribed according to nutrient source and developmental state. This illustrates graphically that growth on a plant represents a particular challenge for pathogens, and attempts to mimic such conditions *in vitro* have so far been unsuccessful (Coleman *et al*., 1997).

Validating predicted genes by expression data

In order to determine a threshold signal above which genes were reliably considered to be expressed, the signals from experimentally determined absent genes were analysed. A genome scan of the nonpathogenic strain Sn79-1087 was obtained using Solexa technology and the reads were compared with the reference SN15 genome. Genes to which no reads mapped were identified and the apparent expression signal of these genes, when probed with cDNA from Sn79-1087, was used to define a background reading. The threshold value was calculated to be 500 on the linear scale and 8.9 on the $\log_2$ scale. A total of 3804 predicted genes fell below the threshold in all of the six conditions tested. This left 12 281 genes with experimental evidence of expression.

These 12 281 genes have been promoted to a SNOG_XXXXX.3 designation. The number of genes predicted to be present in *S. nodorum* is now based on extensive computational, transcriptional and proteogenomic support (Bringans *et al*., 2009; Hane *et al*., 2007). This number of genes is very much as expected by comparison with a range of fungal genomes (Marthey *et al*., 2008).

Differentially expressed genes

Differentially expressed genes were defined as those genes that were expressed in at least one condition (i.e. the expression level average was >500) and showed at least a two-fold difference (with greater than 95% confidence) in expression between two treatments. The various comparisons included the identification of genes differentially expressed between infection and axenic cultures of similar growth stages (3 and 5 dpi *in planta* vs. 4 dpi *in vitro*; late *in planta* vs. 16 dpi *in vitro*), comparison of vegetative and sporulating *in vitro* samples and comparison of samples from various stages of plant infection (Table 1). The earliest time point, 3 dpi, yielded the highest number of differentially regulated genes when compared with the equivalent *in vitro* time point—both up (2105) and down (2981). Only about 30% of these genes had assigned informative gene ontology (GO) terms (Conesa *et al*., 2005; Hane *et al*., 2007). By comparison, 1353 (up) and 1238 (down) genes were regulated in the late time point comparison. The early-expressed, up-regulated, orphan genes could potentially contain additional necrotrophic effector genes alongside *SnToxA* (Friesen *et al*., 2006) and *SnTox3* (Liu *et al*., 2009), which were recently identified in *S. nodorum*. Both *SnTox3* and *SnToxA* are highly expressed early during infection and neither shows meaningful homology to known proteins.

Comparisons (test vs. control)	Significantly higher expression in test	Significantly lower expression in test
3 dpi IP vs. late IP	1693 (372)	2488 (842)
5 dpi IP vs. late IP	189 (29)	232 (64)
3 dpi IP vs. 5 dpi IP	849 (118)	780 (298)
4 dpi IV vs. 16 dpi IV	918 (419)	828 (233)
3 dpi IP vs. 4 dpi IV	2105 (646)	2981 (906)
5 dpi IP vs. 4 dpi IV	1114 (518)	1396 (379)
Late IP vs. 16 dpi IV	1353 (653)	1238 (276)

IP, *in planta*; IV, *in vitro*.

Table 1 Numbers of differentially expressed genes between *in planta* developmental stages, between *in planta* and corresponding *in vitro* samples, and between *in vitro* developmental stages. The various comparisons are listed as a test against a control and the differentially expressed genes are reported as relative to the test. The numbers in parentheses indicate the numbers of differentially expressed genes that have informative gene ontologies.

Expression of genes in biochemical pathways

Scanning the genome sequence for genes associated with enzyme commission (EC) numbers resulted in a list of genes that could be placed into 162 metabolic pathways putatively present in *S. nodorum*. The genes associated with biochemical pathways were cross-referenced against lists of differentially expressed genes (Tables 2 and 3). This provided an analysis of metabolic pathways with genes that were transcriptionally regulated during the life cycle of the fungus. Table 2 shows 57 biochemical pathways that have genes that are differentially expressed between *in planta* and *in vitro* samples. Pathways with at least two genes regulated in at least one comparison are included. This analysis gives a preliminary indication of the activity and direction of a pathway.

The degradative pathways for 4-aminobutyrate, homogalacturonan, melibiose, β-alanine, serine, sorbitol (including genes for pentose catabolism), triacylglycerol and tyrosine were up-regulated *in planta*, as were the biosynthetic pathways for arginine, chorismate, fatty acids, histidine, lysine, ornithine, phenylalanine, purine, spermidine, uridine diphosphate (UDP)-galactose and urate and the nucleoside salvage pathways (Table 2). Conversely, biosynthetic pathways for biotin, choline, cyclopropane fatty acids, formyl-tetrahydrofolate (THF) biosynthesis, glutamate, (iso)leucine and valine, pantothenate and proline were down-regulated *in planta*, together with the degradative pathways for phospholipids (Table 2). The highlighted pathways reflect broad differences in the nutritional environment *in planta* vs. *in vitro*. The *in vitro* medium used contains sucrose, nitrate, phosphate and inorganic micronutrients only. The fungus evidently must synthesize all metabolites from these simple precursors. The *in planta* up-regulated genes indicate that some, but not all, amino acids and other metabolites are not supplied in adequate quantities by the plant. These include the amino acids phenylalanine, tryptophan, arginine and lysine, as well as polyamine and nucleotides. In contrast, the down-regulation of biosynthetic genes for glutamate and the isoleucine/valine family of amino acids, proline and pantothenate (a precursor of CoA) suggests that these are at least partially supplied by the plant. These findings support the notion that the direct source of nitrogen for the fungus *in planta* is mainly glutamate and asparagines (Solomon *et al*., 2003a; Tavernier *et al*., 2007). Other nitrogen sources might include small peptides or amino acids derived from proteolytic cleavage of plant proteins and 4-aminobutyrate (GABA). This is consistent with the expression of genes for amino acid recycling. The observation that the pathway for GABA breakdown was up-regulated during infection is consistent with the hypothesis that various pathogens induce their hosts to produce this stress metabolite, so that it is available for consumption (Oliver and Solomon, 2004; Solomon and Oliver, 2002). We discuss further the pantothenate pathway below. The gene expression profiles suggest the primary carbon sources are simple sugars derived from the breakdown of sucrose, starch and cell wall carbohydrates. The carbohydrate degradation enzymes are also discussed below.

Pathways with more than one co-regulated gene between 3 dpi *in planta* and late *in planta* conditions are highlighted in Table 3. Pathways up-regulated late in infection include biosynthetic pathways for fatty acids and triglycerides, glycogen, ornithine, β-alanine and tetrapyrroles, and degradation pathways for phospholipids and fatty acids, proline, tryptophan, valine and xylitol. In addition, the fermentation of sugars to ethanol and the removal of active oxygen were up-regulated. Pathways up-regulated early in infection include histidine, purine and UDP-*N*-acetyl-D-galactosamine biosynthesis, as well as homogalacturonan and triglyceride degradation. A phase of sulphate assimilation early in infection is replaced by sulphite oxidation later in infection (see also Fig. 5). These changes reflect the need for the biosynthesis of chitin, nucleic acids early in infection and storage compounds at the expense of intermediary metabolites late in infection. The expression of fermentation genes suggests that either oxygen is limiting or that there is a superabundance of carbon relative to nitrogen (and other macronutrients).

These findings are in accordance with previous studies carried out on *S. nodorum* strains deleted for various metabolic genes. Mutants in the nitrate assimilatory pathway (Howard *et al*., 1999) were fully pathogenic, proving that reduced nitrogen sources are adequate for infection. In contrast, mutants in tetrapyrrole (Solomon *et al*., 2006a) and polyamine (Bailey *et al*., 2000) biosynthesis, or the glyoxalate cycle (Solomon *et al*., 2004a), were nonpathogenic.

Table 2 Metabolic pathways with at least two genes that are differentially expressed when *in planta* conditions are compared with the temporally related axenic cultures and when early *in vitro* is compared with late *in vitro*.

	Comparisons between *in planta* and *in vitro* at equivalent developmental stages						Comparisons between *in vitro* developmental stages	
Pathway	3 dpi IP > 4 dpi IV	3 dpi IP < 4 dpi IV	5 dpi IP > 4 dpi IV	5 dpi IP < 4 dpi IV	Late IP > 16 dpi IV	Late IP < 16 dpi IV	4 dpi IV > 16 dpi IV	4 dpi IV < 16 dpi IV
4-Aminobutyrate degradation III (4 genes)	2		1		3			
Arginine biosynthesis II (acetyl cycle) (9 genes)					4		4	
Chorismate biosynthesis (7 genes)			1		2		1	
Cyclopropane fatty acid (CFA) biosynthesis (2 genes)				2				
Ergosterol biosynthesis (6 genes)	2			1	1		1	
Fatty acid biosynthesis—initial steps I (10 genes)		2						
Fatty acid elongation—saturated (25 genes)	5	7	6	1	9	1	4	
Fatty acid β-oxidation II (core pathway) (16 genes)	2	2	1	1	3		2	
Fatty acid β-oxidation IV (unsaturated, even number) (7 genes)					2		1	
Folate polyglutamylation I (5 genes)							2	
Folate transformations (8 genes)		1		1			4	
Gluconeogenesis (13 genes)	2	2			1		1	1
Glutamate biosynthesis III (2 genes)		2		2			2	
Homogalacturonan degradation (5 genes)	2		1		2		1	
Glycogen biosynthesis II (from UDP-D-glucose) (4 genes)		1	1		2			
Glycogen degradation II (5 genes)	2	1	3		3			1
Isoleucine biosynthesis from threonine (13 genes)		4		3	1	2	3	
Isoleucine degradation I (14 genes)		3		3	2	2	2	
L-Arabinose degradation II (1 gene)							1	
L-Cysteine degradation I (6 genes)		1		1		1		
Leucine biosynthesis (10 genes)		3		3		2	1	
Leucine degradation I (13 genes)		3	1	3	1	2	1	
L-Serine degradation (2 genes)					2		2	
Lysine biosynthesis IV (6 genes)	2		1		2		3	1
Melibiose degradation (4 genes)	2		2		2			
Methionine degradation I (to homocysteine) (4 genes)		2			2		2	
Nitrate reduction V (assimilatory) (7 genes)		4		2			4	
Ornithine biosynthesis (6 genes)			2		3		3	
Oxidative ethanol degradation I (22 genes)	6	4	5	2	8	1	1	1
Pantothenate biosynthesis I (10 genes)		4		4		4	1	1
Phenylalanine biosynthesis I (4 genes)	1				2		2	
Phospholipases (8 genes)		3				1		
Proline biosynthesis I (7 genes)		2		2			2	
Purine nucleotides *de novo* biosynthesis II (11 genes)	3		1		2		3	
Pyruvate fermentation to ethanol II (17 genes)	5	4	3	3	6	2	1	1
Removal of superoxide radicals (9 genes)		1	1	1	2			1
S-Adenosyl-L-methionine cycle (4 genes)		2			2		3	
Salvage pathways of adenine, hypoxanthine and their nucleosides (5 genes)	2		2					1
Sorbitol utilization (5 genes)	4		4		4		1	
Spermidine biosynthesis (2 genes)	2		1		1			
β-Alanine biosynthesis V (8 genes)	1	1	2		2	1		
β-Alanine degradation I (3 genes)	2		1		2			
Sucrose degradation to ethanol and lactate (anaerobic) (25 genes)	5	6	3	4	6	3	3	1
Sulphite oxidation IV (3 genes)		1	1		2			
Tetrapyrrole biosynthesis II (5 genes)	1	2			1		1	
Trehalose degradation II (trehalase) (5 genes)	1	3	1	1	1			
Triacylglycerol biosynthesis (8 genes)	1	3						
tRNA charging pathway (25 genes)		2			1		1	
Tryptophan degradation to 2-amino-3-carboxymuconate semialdehyde (4 genes)	2	1		1	2	1		2
Tryptophan degradation VI (via tryptamine) (8 genes)	5	1	3	1	3		1	
Tyrosine degradation I (7 genes)	1		2		5			1
UDP-*N*-Acetyl-D-galactosamine biosynthesis II (4 genes)	2		1					
Urate biosynthesis (5 genes)	2		2					1
Valine biosynthesis (12 genes)		4		3	1	2	3	
Valine degradation II (24 genes)	5	7	3	6	6	4	2	1
Xylitol degradation (4 genes)	1	2	1		1			

UDP, uridine diphosphate.

Table 3 Metabolic pathways that have at least two genes that are differentially expressed when *in planta* conditions are compared.

Pathway	3 dpi IP > late IP	3 dpi IP < late IP
Choline biosynthesis III (4 genes)		2
Fatty acid biosynthesis—initial steps I (10 genes)		2
Fatty acid elongation—saturated (25 genes)	2	6
Fatty acid β-oxidation II (core pathway) (16 genes)		4
Glycogen biosynthesis II (from UDP-D-glucose) (4 genes)		2
Histidine biosynthesis I (7 genes)	3	
Homogalacturonan degradation (5 genes)	2	
Ornithine biosynthesis (6 genes)		2
Oxidative ethanol degradation I (22 genes)	1	5
Phospholipases (8 genes)		4
Proline degradation I (3 genes)		2
Purine nucleotides *de novo* biosynthesis II (11 genes)	5	
Pyruvate fermentation to ethanol II (17 genes)	1	3
Removal of superoxide radicals (9 genes)	1	2
Salvage pathways of adenine, hypoxanthine and their nucleosides (5 genes)	2	1
β-Alanine biosynthesis V (8 genes)		3
Sucrose degradation to ethanol and lactate (anaerobic) (25 genes)	1	5
Sulphate reduction I (assimilatory) (5 genes)	3	
Sulphite oxidation IV (3 genes)		2
TCA cycle variation III (eukaryotic) (12 genes)		2
Tetrapyrrole biosynthesis II (5 genes)		2
Triacylglycerol biosynthesis (8 genes)		2
Triacylglycerol degradation (25 genes)	6	7
tRNA charging pathway (25 genes)		2
Tryptophan degradation to 2-amino-3-carboxymuconate semialdehyde (4 genes)	1	2
Tryptophan degradation VI (via tryptamine) (8 genes)	2	
Tyrosine degradation I (7 genes)		4
UDP-*N*-Acetyl-D-galactosamine biosynthesis II (4 genes)	2	
Valine degradation II (24 genes)	1	3
Xylitol degradation (4 genes)		2

TCA, tricarboxylic acid; UDP, uridine diphosphate.

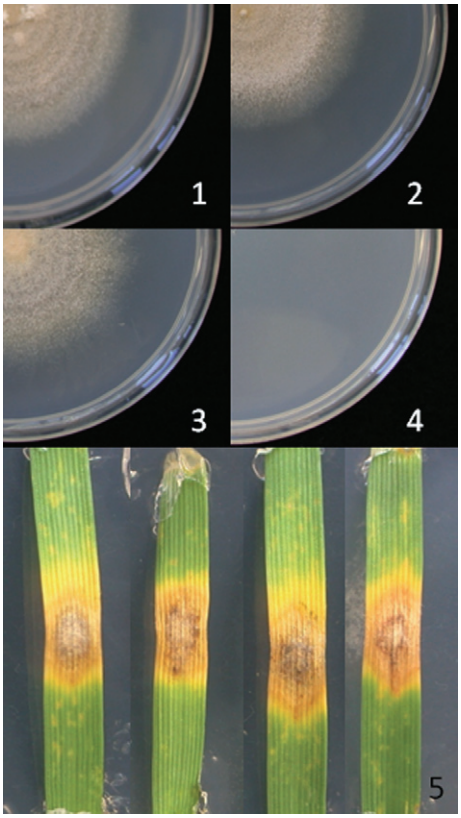

Fig. 3 Growth of SN15 (1 and 2) and the *Pbl1* deleted strain (3 and 4) on minimal medium with (1 and 3) and without (2 and 4) added pantothenate. Detached leaf assay (5, from left to right) of two *Pbl1* strains and ectopic and wild-type control.

Pantothenate biosynthesis

Pantothenate is the first committed precursor in the biosynthesis of CoA, an essential co-factor used in numerous central metabolic pathways (Spry *et al*., 2008). The *in vitro* requirement to synthesize CoA is reflected in the high expression level of the biosynthetic genes (Table 2). Our expectation was that these genes would be expressed at a similar level *in planta*. Genes in the pathway were expressed at lower levels *in planta*, suggesting a lower demand for the *de novo* synthesis of panthothenate *in planta* vs. *in vitro* (Table 2). To investigate this further, we ablated *SNOG_08736.3*, a gene with homology to pantothenate-β-alanine ligase *Pbl1* (EC6.3.2.1). Two independent mutants were isolated. The mutants failed to grow on minimal medium unless supplemented with 10 mM panthothenate. This confirmed the identity of the enzyme encoded by SNOG_08736 (Fig. 3). The growth rate of the mutants was unaltered from the wild-type on complete and supplemented medium. The pathogenicity of the strains was tested by detached leaf and whole-seedling assays (Solomon *et al*., 2003b). Surprisingly, pathogenicity was not significantly affected in detached leaf assays (Fig. 3) or when entire plants were infected (data not shown). It therefore appears that fungal pantothenate biosynthesis is dispensable for growth in plants, and that *S. nodorum* can assimilate CoA or a precursor. It remains to be seen whether the host plant supplies pantothenate or a later intermediate in the pathway. The ability of the fungus to assimilate aminolevulinate from the host has been noted previously (Solomon *et al*., 2006a). We have noted further that biotin biosynthesis is down-regulated *in planta*. If these findings prove to apply to other fungi, the uptake and conversion of intermediary metabolites, such as alanine and pantothenate, might prove to be valuable fungicide targets.

Other regulated metabolic pathways

Ergosterol is a sterol that is part of the fungal cell membrane and has been used to quantify fungal biomass (Gessner, 2005; Manuela, 2009). The ergosterol biosynthesis pathway has been a

major focus for fungicide development, mainly targeting the *CYP51* genes (Blixt *et al*., 2009; Knight *et al*., 1997). The expression pattern showed that the transcription of ergosterol biosynthesis-related enzymes was mostly down-regulated towards the latter stages of the fungal life cycle (Fig. 4). This pattern of declining expression (note the logarithmic scale) is consistent with the typical growth curve of fungal pathogens and slower growth rates towards sporulation. Although two *CYP51* (Erg11) genes were identified, only *SNOG_03702.3* had an elevated expression. *SNOG_04607* was not expressed above the threshold, except marginally at 4 dpi *in vitro*, and may be a pseudogene. Fungicide resistance has been studied in *S. nodorum*, but no changes in CYP51 genes were noted (Blixt *et al*., 2009).

The genes associated with sulphur metabolism showed striking regulation. (Fig. 5A,B). Five sulphate permease genes were identified. Two, *SNOG_14281.3* and *SNOG_04510.3*, were highly expressed during the early stages of infection, whereas all five were highly expressed later in infection, as well as during *in vitro* growth. This suggests that the pathogen avidly scavenges sulphate during the early stages of infection and converts it into sulphur-containing amino acids and proteins (Fig. 5B). Sulphite oxidase converts sulphite (presumably derived from degraded cysteine) to sulphate and peroxide. The pronounced differential expression of one sulphite oxidase gene (*SNOG_13212.3*) late in infection suggests that amino acid catabolism is a significant energy resource, with the consequent need to remove and detoxify reactive –SH and sulphite residues. Cyprodinil is a fungicide that is believed to target sulphur assimilation. Furthermore, the decline of *S. nodorum* as a pathogen in the UK has been linked to the reduction in sulphate pollution levels (Bearchell *et al*., 2005). It is conceivable that the manipulation of the sulphur status of the plant or of sulphur metabolism in the fungus could help to control disease levels.

Inorganic phosphate plays a vital role in the synthesis of nucleic acids, phospholipids and co-factors (Wykoff and O'Shea, 2001). In *S. nodorum*, genes encoding phosphate transporters (*SNOG_12371.3*, *SNOG_15532.3*, *SNOG_08757.3* and *SNOG_05237.3*) were generally expressed at high levels during the early stages of

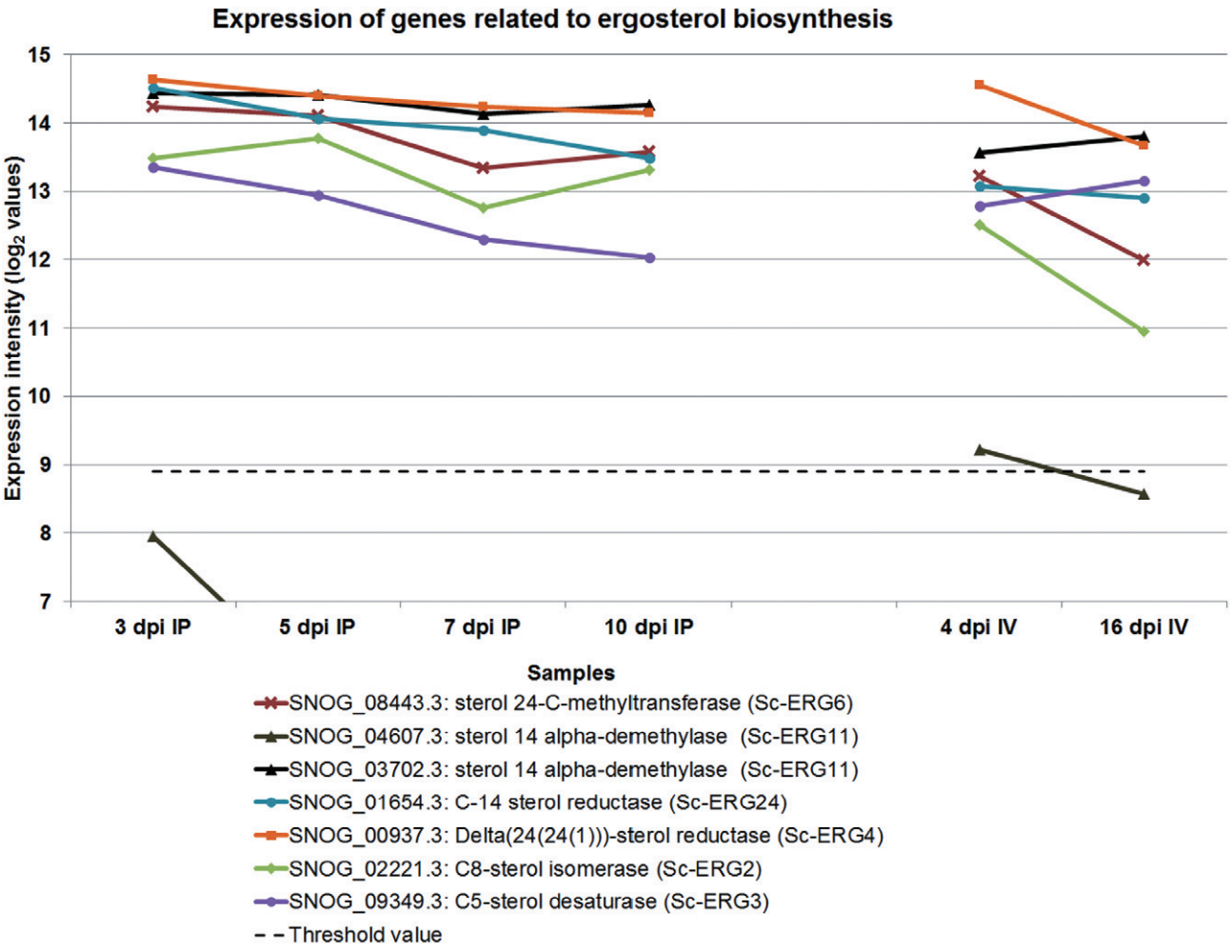

Fig. 4 The expression of *CYP51* genes and other regulated genes involved in ergosterol biosynthesis. IP, *in planta*; IV, *in vitro*.

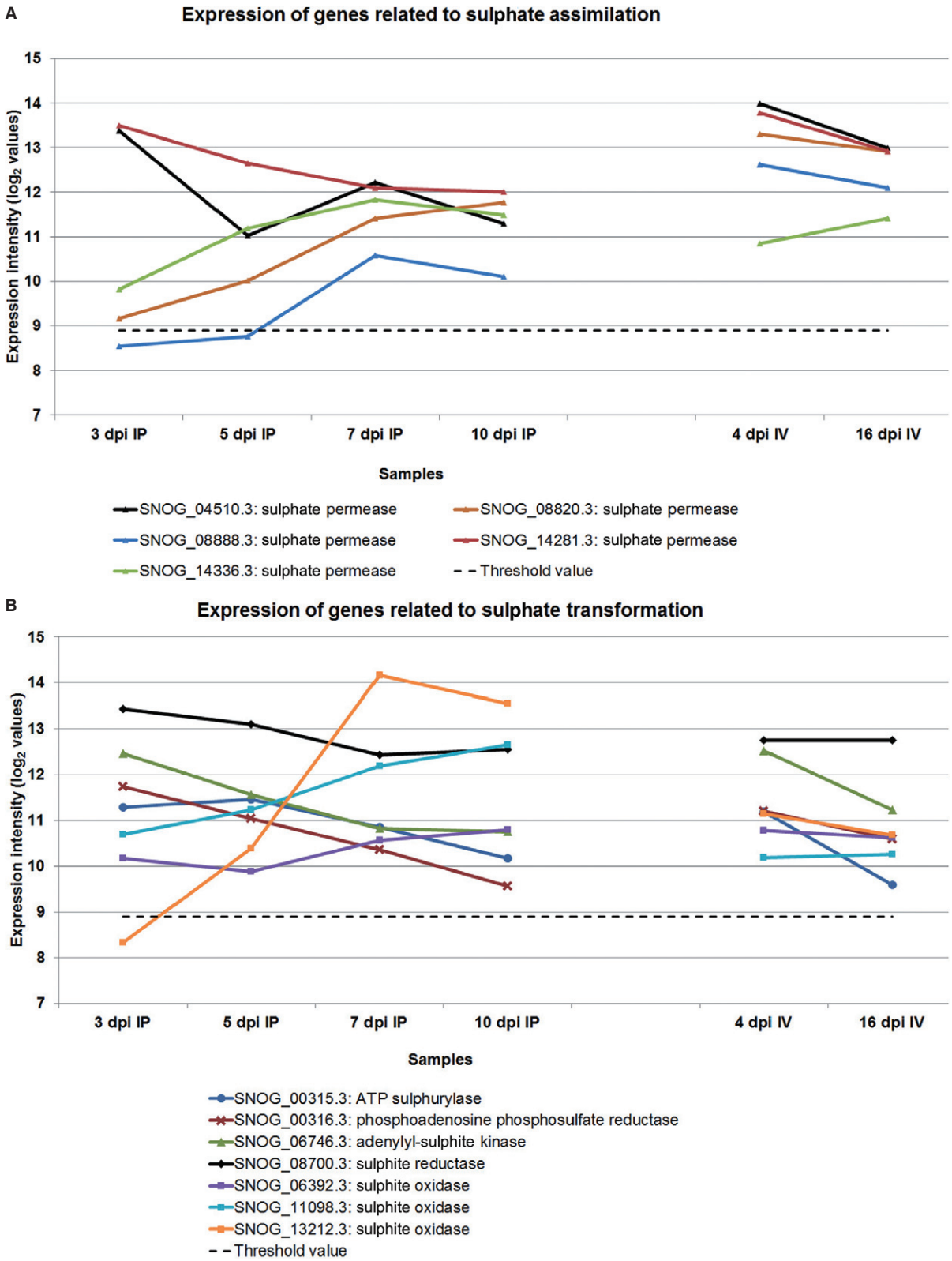

Fig. 5 The expression level of genes responsible for the assimilation of sulphate (A) and the conversion of sulphates (B). IP, *in planta*; IV, *in vitro*.

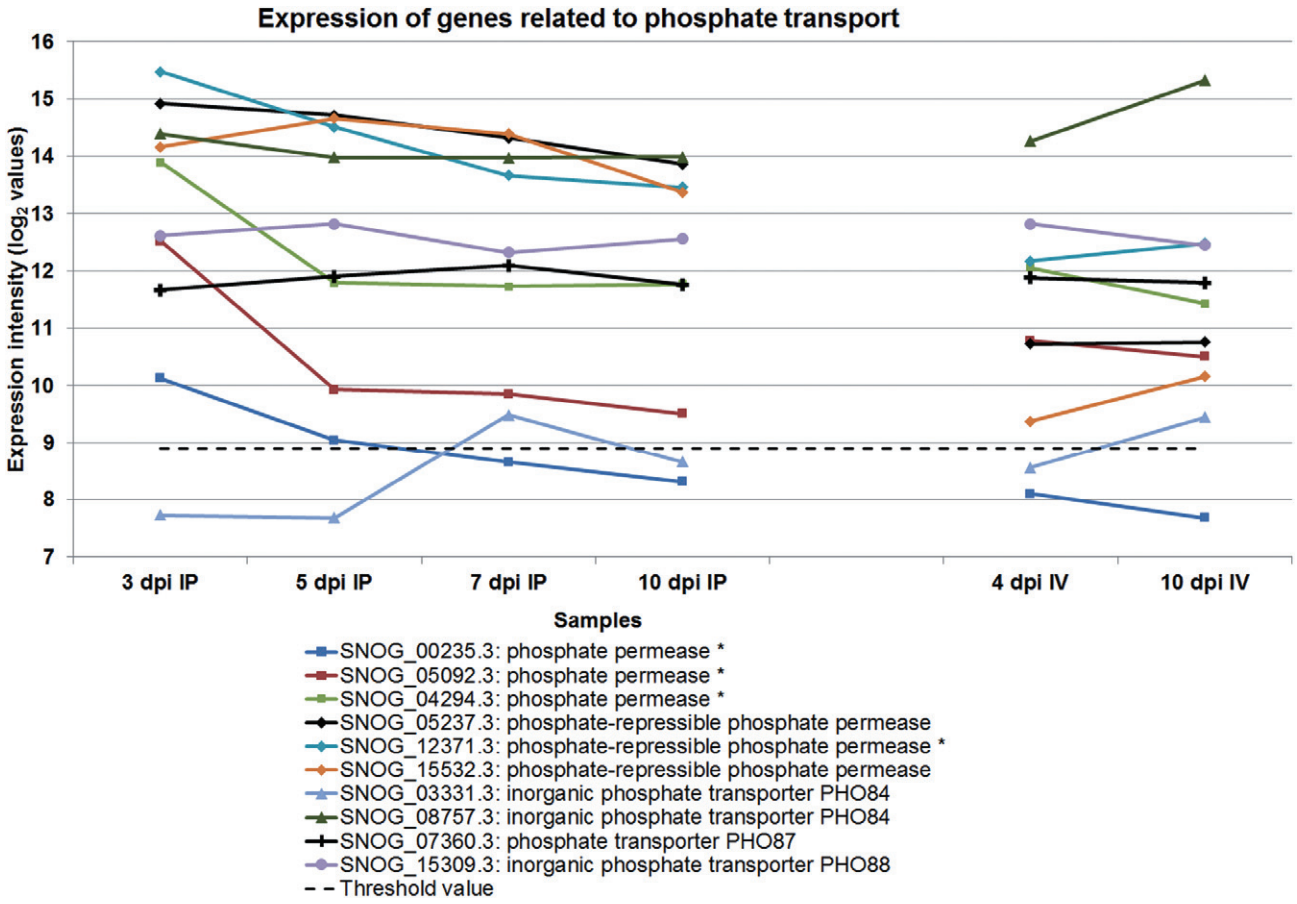

Fig. 6 The expression of genes encoding phosphate transporters. IP, *in planta*; IV, *in vitro*.

infection, but declined to lower levels during the later stages of infection (Fig. 6). The data suggest the avid uptake of inorganic phosphates from the host during the early stages of infection to support metabolism and also potentially for phosphate storage as polyphosphates (Cramer and Davis, 1984). Phosphate-repressible phosphate permeases and *PHO84* were transcriptionally up-regulated during phosphate limitation (Bun-Ya *et al*., 1991; Persson *et al*., 1998). As a down-regulation was observed towards the end of infection, it is possible that sufficient inorganic phosphates were accumulated and negative feedback led to lower levels of transcription for these genes. In contrast with the *in planta* conditions, the expression of the inorganic phosphate transporters *PHO84* and phosphate-repressible phosphate permeases *in vitro* was up-regulated during sporulation *in vitro* (Fig. 6). Phosphates were supplied in the form of sodium phosphate salts in minimal medium and were readily available. However, after 16 days of growth, supplies of inorganic phosphates would be scarce, leading to the increased transcription of these transporters to boost phosphate uptake. Although phosphate transporters have been studied extensively in yeast (Persson *et al*., 1998), *Neurospora crassa* (Versaw, 1995) and biotrophic fungi (Hahn and Mendgen, 2001), there is no report regarding phosphate transporter studies in necrotrophic fungi. This study showed that phosphate transporters are important during the early stages of pathogenicity and opened up new avenues for pathogenicity studies.

There were multiple copies of genes involved in the catabolism of phenylalanine and tyrosine, and many were expressed at very high levels. Furthermore, they were up-regulated during sporulation *in planta* (Fig. 7). Phenylalanine is degraded by a series of enzymes to produce fumarate and acetoacetate. The catabolic pathway has been studied intensively in *Aspergillus nidulans* (Fernández-Cañón and Peñalva, 1995, 1998; da Silva Ferreira *et al*., 2006). The biosynthesis of aromatic amino acids is very active and they have been shown to be precursors of the dihydroxyphenylalanine (DOPA)–melanin pathway (Solomon *et al*., 2004b). We speculate that the over-production of these amino acids occurs, resulting in the need to recycle them late during infection.

Unlike the DOPA–melanin pathway, which has so far only been demonstrated in *S. nodorum* amongst plant pathogens (Solomon *et al*., 2004b), the 1,8-dihydroxynaphthalene (DHN)–melanin

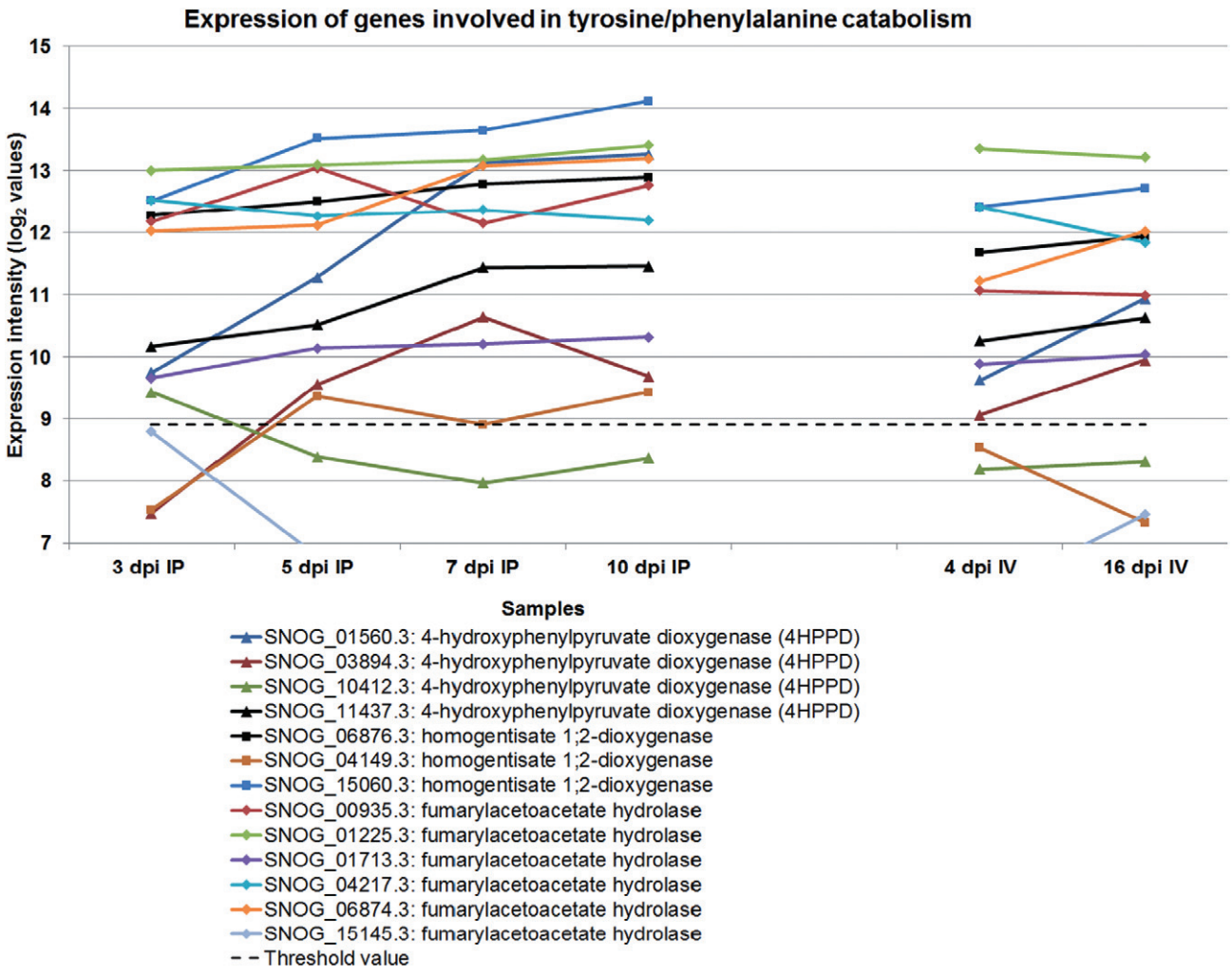

Fig. 7 The expression profile of genes encoding enzymes responsible for the catabolism of phenylalanine and tyrosine. IP, *in planta*; IV, *in vitro*.

biosynthesis pathway is widely distributed and exploited as a target for fungicides, such as tricyclazole (Butler and Day, 1998; Langfelder *et al*., 2003). The presence and expression of genes in the DHN pathway demonstrate that both melanin biosynthesis pathways are active. Most of the genes involved in this pathway were up-regulated during infection, consistent with the need for melanin during sporulation (Fig. 8).

Carbohydrate active enzyme (CAZy) analysis

We have analysed the genes encoding the enzymes that assemble (glycosyltransferases, GTs) and degrade (glycoside hydrolases, GHs) complex carbohydrates, and compared *S. nodorum* with *M. graminicola* IPO323 (Table 4) (Goodwin *et al*., 2011). Although the two fungi have a very comparable GT content, *S. nodorum* has many more enzymes than *M. graminicola* for the cleavage of complex carbohydrates (287 vs. 194 GHs). Interestingly, the differences between the two fungi appear to be concentrated in enzyme families that are implicated in cellulose and xylan breakdown, namely families GH6, GH7, GH10, GH11, GH12, GH45 and GH61, where *S. nodorum* has a total of 60 genes and *M. graminicola* has only eight. This is particularly pronounced in family GH61, where *S. nodorum* has 30 genes and *M. graminicola* has only two. This is very consistent with the difference in pathogenicity of the two species. *Stagonospora nodorum* causes necrosis with no apparent latent phase (Solomon *et al*., 2006d). The observed tissue collapse is consistent with the expression of large numbers of cellulases and xylanases. Infection by *M. graminicola* is much slower and involves a long latent period (Keon *et al*., 2005). Significantly, all *S. nodorum* GH7 (cellulases) and most GH11 (xylanases) were found to be induced *in planta*.

Only a few CAZy families are more abundant in *M. graminicola* than in *S. nodorum*: GH13 and GT5. These two families share the two constitutive domains of α-glucan synthase, an enzyme that produces fungal cell wall α-glucans. *Mycosphaerella graminicola* has four such α-glucan synthases, whereas *S. nodorum* has none.

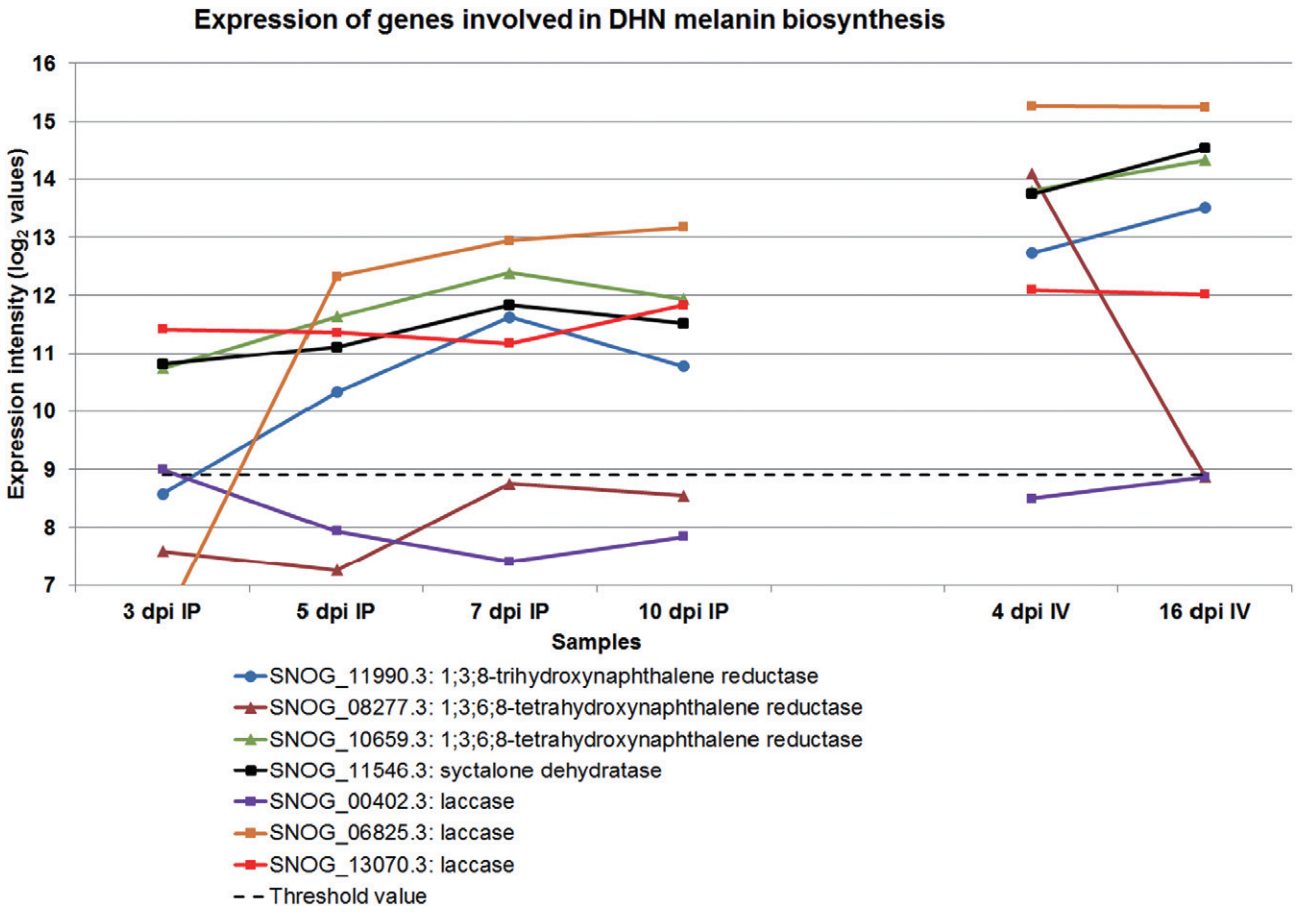

Fig. 8 The expression profile of genes encoding enzymes involved in the biosynthesis of melanin. DHN, 1,8-dihydroxynaphthalene; IP, *in planta*; IV, *in vitro*.

Table 4 Difference in carbohydrate active enzyme (CAZy) gene complements in *Mycosphaerella graminicola* and *Stagonospora nodorum*. Full list is given in Supporting Information.

	GT family		GH family								
	Total	GT5	Total	GH6	GH7	GH10	GH11	GH12	GH13	GH45	GH61
Mycosphaerella graminicola IPO323	97	14	194	0	1	2	1	1	14	1	2
Stagonospora nodorum SN15	92	7	287	4	5	7	7	4	7	3	30

GH, glycoside hydrolase; GT, glycosyltransferase.

In summary, our microarray experiment has detected significant gene expression of more than 12 000 genes during one or more of four *in planta* and two *in vitro* time points. This provides strong evidence for the validity of these gene models. Very large numbers of genes are differentially expressed. A substantial number of genes without obvious homologues in other species are differentially or exclusively expressed in the early stage of plant infection. These genes may include further necrotrophic effectors required for virulence on specific wheat genotypes. We focused on genes with annotated roles in metabolism. The picture that emerged is one of tightly coordinated expression regulated by both fungal age and environment. Unravelling the roles of many of these genes and pathways will be a significant challenge, but one which promises to further increase the control of this important fungus (Oliver, 2008) and its relatives in the Dothideomycetes.

EXPERIMENTAL PROCEDURES

Biological materials

Stagonospora nodorum strain SN15 (Solomon *et al*., 2006c) was grown and wheat (cv. Amery) leaves were infected as described previously. At 3, 5, 7 and 10 dpi, lesions were collected in biological triplicates. The developed lesions were excised using sterile scissors to maximize fungal material and reduce interference from plant material. The lesions corresponding to the key stages of infection were transferred into 10-mL plastic tubes

(Sarstedt, Adelaide, Australia), frozen under liquid nitrogen and stored at −80 °C for later use.

Axenic *in vitro* culture for RNA isolation

Stagonospora nodorum strain SN15 was grown on minimal medium (Solomon *et al*., 2003b). Fungal tissues were collected at 4 and 16 dpi in triplicates for RNA collection. The avirulent strain Sn79-1087 (Friesen *et al*., 2006) was also grown in duplicate at 4 dpi for RNA collection. The tissues were snap frozen in liquid nitrogen and stored at −80 °C until processed.

RNA extraction and clean up

Tissues were ground to a fine powder under liquid nitrogen using a mortar and pestle that had been baked overnight at 150 °C. RNA was extracted from the ground tissue according to Solomon *et al*. (2006c) using Trizol Reagent (Invitrogen, Carlsbad, CA, USA). The precipitated RNA was resuspended in 30 μL of diethylpyrocarbonate (DEPC)-treated water. RNA concentrations were determined using a NanoDrop instrument (Thermo Scientific Inc., NanoDrop Products, Wilmington, DE, USA). Contaminating gDNA in the RNA samples was removed using DNA-free reagent (Ambion, Austin, TX, USA), following the manufacturer's instructions. The efficiency of the treatment was evaluated by PCR using the treated samples with primers designed for fungal actin and/or intron-spanning primers (actinqPCRF, 5′-AGTCGAAGCGTGGTATCCT-3′; actinqPCRR, 5′-ACTTGGGGTTGATGGG AG-3′). The DNase-treated RNA was cleaned according to the manufacturer's instructions using a Qiagen RNeasy Kit (Qiagen, Valencia, CA, USA).

RNA integrity and quality assessment

The quality and integrity of RNA samples for microarray analysis were assessed using an Agilent Bioanalyzer 2000 (Agilent, Santa Clara, CA, USA). The samples were processed according to the manufacturer's instructions and the resulting electropherograms were analysed for RNA integrity.

Microarray-related experimentation

Good-quality total RNA was sent to Roche-NimbleGen Inc. (Reykjavik, Iceland) for microarray-related experiments. As part of their service, Roche-NimbleGen produced double-stranded cDNA from the supplied RNA using a SuperScript™ Double-Stranded cDNA Synthesis Kit (Invitrogen, Carlsbad, CA, USA). The double-stranded cDNA was labelled using the Roche-NimbleGen One-Color DNA Labeling Kit (Madison, WI, USA). Four micrograms of the Cy3-labeled cDNA sample were used for each of the hybridizations.

The *S. nodorum* genome sequence (Hane *et al*., 2007) was used by Roche-NimbleGen (Madison, WI, USA) to design and synthesize four-plex arrays with 72 000 features per hybridization zone onto standard glass microscope slides. For each gene, three to four 60-oligomer probes were designed in the 2-kbp exonic region from the 3′ end of the gene, and a total of 16 085 genes was synthesized per zone. Roche-NimbleGen also carried out hybridization of the arrays with Cy3-labelled cDNA, scanning and data extraction as part of their gene expression array service. Thus, for the virulent SN15 strain, data were collected from the biological triplicates of each infection time point and axenic culture, and in duplicate for the axenic culture of the avirulent SN79-1087 strain.

Normalization of the array data

Chip to chip normalization was performed using data from one chip as a reference. Data from all the other arrays were normalized according to the reference chip to allow cross-array comparisons. The data were processed by Roche-NimbleGen using quantile normalization (Bolstad *et al*., 2003) from the Bioconductor software package (http://www.bioconductor.org) and the Robust Multi-chip Average (RMA) algorithm (Irizarry *et al*., 2003).

Quality control of gene expression data from microarrays

To assess the efficiency of the normalized data, box plots were created using the JMP7 statistical package. The box plots were used to provide visual comparisons between the various $\log_2$-transformed datasets (Fig. S2, see Supporting Information). Furthermore, the expression pattern of three genes was cross-checked using qRT-PCR to ascertain the reliability of the data (Fig. S2). cDNAs were produced from total RNA using the Bio-Rad iScript cDNA Synthesis Kit, according to the manufacturer's instructions (Bio-Rad, Hercules, CA, USA). Conditions for qRT-PCR were as described in Solomon *et al*. (2006c). The following primers were used: SNOG16152 qPCRF, 5′-GTTTCAGGTGTATGCAAGGT-3′; SNOG16152qPCRR, 5′-TAGCA GTAGATCACCAGGCT-3′; Tox3qPCRF, 5′-AATGTCGACCGTTTTGACC-3′; Tox 3qPCRR, 5′-GGTTGCCGCAGTTGATATAA-3′; SNOG14941qPCRF, 5′-TCAGA CACCGCAAGGTA-3′; SNOG14941qPCRF, 5′-TCTTGGTATATCCGCTGTCT-3′.

Principal component analysis

Principal component analysis was used to visualize and conceptualize the microarray data in two dimensions. It was performed using The Unscrambler® software developed by CAMO software AS (http://www.camo.com). Prior to principal component analysis, the microarray data were transformed by normalization using the software's inbuilt algorithm. The expression values from each condition were divided by the mean value, so that the influence of any hidden factor was neutralized.

Establishment of a threshold value for gene expression

To generate a control set, an *S. nodorum* strain that was essentially non-pathogenic on wheat (Sn79-1087) (Friesen *et al*., 2006) was sequenced by Solexa technology (2–3× genome scan; data not shown; a more extensive sequencing procedure has been carried out and will be published separately) and the sequence reads were compared with the reference SN15 genome; 112 SN15 genes for which no sequences were found in the Sn79-1087 reads were considered to be absent in this nonpathogenic strain (Table S1, see Supporting Information). The apparent microarray intensity, when probed with RNA from Sn79-1087, was used to define a background reading. A conservative threshold value was defined by adding twice the standard deviation to the highest expression value of

the 112 genes, thus ensuring that the threshold value for expression was statistically robust and conservative. The threshold value was calculated to be 500 on the linear scale and 8.9 on the $\log_2$ scale.

Analysis of differentially expressed genes

The array data were analysed using the Arraystar® software package (http://www.dnastar.com). The scatter plot function was used to select for genes that were differentially expressed between the transcriptomic profile of two samples. Genes were defined as differentially expressed if the expressed genes had a fold change equal to or greater than two and if the moderated *t*-test produced a *P* value of less than or equal to 0.05, after the application of a Benjamini–Hochberg false-discovery rate multiple-testing correction (Benjamini and Hochberg, 1995).

Data mining and genome-related information

Data manipulation was performed using the Microsoft Office suite (Microsoft, Redmond, WA, USA) and the Venn diagram generator VENNY (http://bioinfogp.cnb.csic.es/tools/venny/index.html).

Information related to the genome sequence was as described in the published *S. nodorum* genome sequence (Hane *et al*., 2007) has been updated and submitted to the Broad and JGI websites http://genome.jgi-psf.org/programs/fungi/index.jsf and http://www.broadinstitute.org/annotation/genome/stagonospora_nodorum/MultiHome.html. However, we remind the community that the data at the Broad website have not been updated. The updated list of well-supported genes and associated FASTA files is available from the corresponding author.

CAZy analysis

The *S. nodorum* protein models were analysed and assigned to families by the combination of BLAST and HMM searches used for the update of the CAZy database (Cantarel *et al*., 2009; PMID 18838391).

Metabolic pathway analysis

Information related to various biochemical pathways was obtained from the Kyoto Encyclopaedia of Genes and Genomes (KEGG: http://www.genome.jp/kegg/) or from the Encyclopaedia of Metabolic Pathways (MetaCyc: http://metacyc.org/). The genome sequence was used to reconstruct potential metabolic pathways present in *S. nodorum*. Genes in the genome were searched against a database of known enzymes with EC numbers, and these genes were then grouped into biochemical pathways (MetaCyc). From the whole list of biochemical pathways generated, those thought to be present in *S. nodorum* were selected on the basis of previous work in the pathogen and the cross-referencing of well-supported biochemical pathways in *Aspergillus niger* (Andersen *et al*., 2008).

The genes from the biochemical pathways thought to be present in *S. nodorum* were cross-referenced with the expression data from the microarray experiment to generate the metabolic expression dataset. Differentially expressed genes (Fig. 4 and Table 1) were assigned to metabolic pathways to identify which pathways were prominently active during the life cycle of the pathogen.

Deletion of SNOG_08736

The deletion construct was obtained by fusing the flanking regions of SNOG_08736 to the phleomycin resistance cassette (Figs S3 and S4, see Supporting Information). The construct was cloned into the pGEM-T vector and transformed into *Escherichia coli*. A plasmid with the desired construct was used as a template to amplify the deletion construct. *Stagonospora nodorum* was transformed with the deletion via homologous recombination (Solomon *et al*., 2006c). Forty-one transformants were obtained and screened. The screening primers were designed to generate a 4272-bp PCR product from mutants with successful gene deletion and a 2882-bp PCR product from ectopics. The copy number of the deletion construct in the selected transformants was determined by qPCR (Solomon *et al*., 2008). Two of the selected transformants had a single copy insertion and were named KO 08736-1 and KO 08736-35, and one ectopic strain, KO08736-23e, was chosen as a control strain for subsequent testing.

Phenotypic characterization

The mutants were grown on complete V8PDA medium and minimal medium complemented with 10 mM pantothenate, as well as without pantothenate. Whole-plant spray assays (Solomon *et al*., 2003b) were used to investigate the virulence of *pbl1*ins on plants and to determine the requirement of the *Pbl1* gene for pathogenicity. Fourteen-day-old plant seedlings were inoculated with spores of the two *pbl1* mutants, the ectopic strain, the wild-type and a mock infection. The seedlings were exposed to humidity for 48 h. The plants were rated at 7 dpi.

ACKNOWLEDGEMENTS

This research was supported by the Australian Grains Research and Development Corporation through grant UMU00022. We thank Professor Dave Berger for scientific input.

REFERENCES

Andersen, B., Dongo, A. and Pryor, B.M. (2008) Secondary metabolite profiling of *Alternaria dauci, A. porri, A. solani*, and *A. tomatophila*. *Mycol. Res.* **112**, 241–250.

Bailey, A., Mueller, E. and Bowyer, P. (2000) Ornithine decarboxylase of *Stagonospora (Septoria) nodorum* is required for virulence toward wheat. *J. Biol. Chem.* **275**, 14 242–14 247.

Bearchell, S.J., Fraaije, B.A., Shaw, M.W. and Fitt, B.D.L. (2005) Wheat archive links long-term fungal pathogen population dynamics to air pollution. *Proc. Natl. Acad. Sci. USA*, **102**, 5438–5442.

Benjamini, Y. and Hochberg, Y. (1995) Controlling the false discovery rate: a practical and powerful approach to multiple testing. *J. R. Stat. Soc. Ser. B (Methodol.)* **57**, 289–300.

Blixt, E., Djurle, A., Yuen, J. and Olson, Ã. (2009) Fungicide sensitivity in Swedish isolates of *Phaeosphaeria nodorum*. *Plant Pathol.* **58**, 655–664.

Bolstad, B.M., Irizarry, R.A., Astrand, M. and Speed, T.P. (2003) A comparison of normalization methods for high density oligonucleotide array data based on variance and bias. *Bioinformatics*, **19**, 185–193.

Breakspear, A. and Momany, M. (2007) The first fifty microarray studies in filamentous fungi. *Microbiology*, **153**, 7–15.

Brefort, T., Doehlemann, G., Mendoza-Mendoza, A., Reissmann, S., Djamei, A. and Kahmann, R. (2009) *Ustilago maydis* as a pathogen. *Annu. Rev. Phytopathol.* **47**, 423–445.

Bringans, S., Hane, J.K., Casey, T., Tan, K.C., Lipscombe, R., Solomon, P.S. and Oliver, R.P. (2009) Deep proteogenomics; high throughput gene validation by

multidimensional liquid chromatography and mass spectrometry of proteins from the fungal wheat pathogen *Stagonospora nodorum*. *BMC Bioinformatics*, **10**, 301.

Bun-Ya, M., Nishimura, M., Harashima, S. and Oshima, Y. (1991) The PHO84 gene of *Saccharomyces cerevisiae* encodes an inorganic phosphate transporter. *Mol. Cell. Biol.* **11**, 3229–3238.

Butler, M.J. and Day, A.W. (1998) Fungal melanins: a review. *Can. J. Microbiol.* **44**, 1115–1136.

Cantarel, B.L., Coutinho, P.M., Rancurel, C., Bernard, T., Lombard, V. and Henrissat, B. (2009) The Carbohydrate-active EnZymes database (CAZy): an expert resource for glycogenomics. *Nucleic Acids Res.* **37**, D233–D238.

Coleman, M., Henricot, B., Arnau, J. and Oliver, R.P. (1997) Starvation-induced genes of the tomato pathogen *Cladosporium fulvum* are also induced during growth in planta. *Mol. Plant–Microbe Interact.* **10**, 1106–1109.

Conesa, A., Gotz, S., Garcia-Gomez, J.M., Terol, J., Talon, M. and Robles, M. (2005) Blast2GO: a universal tool for annotation, visualization and analysis in functional genomics research. *Bioinformatics*, **21**, 3674–3676.

Cramer, C.L. and Davis, R.H. (1984) Polyphosphate-cation interaction in the amino acid-containing vacuole of *Neurospora crassa*. *J. Biol. Chem.* **259**, 5152–5157.

Dean, R.A., Talbot, N.J., Ebbole, D.J., Farman, M.L., Mitchell, T.K., Orbach, M.J., Thon, M., Kulkarni, R., Xu, J.R., Pan, H., Read, N.D., Lee, Y.I., Carbone, I., Brown, D., Yeon, Y.O., Donofrio, N., Jun, S.J., Soanes, D.M., Jonovic, S.D., Kolomlots, E., Rehmeyer, C., Li, W., Harding, M., Kim, S., Lebrun, M.H., Bohnert, H., Coughlan, S., Butler, J., Calvo, S., Ma, L.J., Nicol, R., Purcell, S., Nusbaum, C., Galagan, J.E. and Birre, B.W. (2005) The genome sequence of the rice blast fungus *Magnaporthe grisea*. *Nature*, **434**, 980–986.

Donofrio, N.M., Oh, Y., Lundy, R., Pan, H., Brown, D.E., Jeong, J.S., Coughlan, S., Mitchell, T.K. and Dean, R.A. (2006) Global gene expression during nitrogen starvation in the rice blast fungus, *Magnaporthe grisea*. *Fungal Genet. Biol.* **43**, 605–617.

Eichhorn, H., Lessing, F., Winterberg, B., Schirawski, J., Kamper, J., Muller, P. and Kahmann, R. (2006) A ferroxidation/permeation iron uptake system is required for virulence in *Ustilago maydis*. *Plant Cell*, **18**, 3332–3345.

Ellwood, S.R., Liu, Z., Syme, R.A., Lai, Z., Hane, J.K., Keiper, F., Moffat, C.S., Oliver, R.P. and Friesen, T.L. (2010) A first genome assembly of the barley fungal pathogen *Pyrenophora teres* f. *teres*. *Genome Biol.* **11**, R109.

Faris, J.D., Zhang, Z., Lu, H., Lu, S., Reddy, L., Cloutier, S., Fellers, J.P., Meinhardt, S.W., Rasmussen, J.B., Xu, S.S., Oliver, R.P., Simons, K.J. and Friesen, T.L. (2010) A unique wheat disease resistance-like gene governs effector-triggered susceptibility to necrotrophic pathogens. *Proc. Natl. Acad. Sci. USA*, **107**, 13 544–13 549.

Fernández-Cañón, M.J. and Peñalva, M.A. (1995) Molecular characterization of a gene encoding a homogentisate dioxygenase from *Aspergillus nidulans* and identification of its human and plant homologues. *J. Biol. Chem.* **270**, 21 199–21 205.

Fernández-Cañón, J.M. and Peñalva, M.A. (1998) Characterization of a fungal maleylacetoacetate isomerase gene and identification of its human homologue. *J. Biol. Chem.* **273**, 329–337.

Friesen, T.L., Rasmussen, J.B., Kwon, C.Y., Ali, S., Francl, L.J. and Meinhardt, S.W. (2002) Reaction of Ptr ToxA-insensitive wheat mutants to *Pyrenophora tritici-repentis* race 1. *Phytopathology*, **92**, 38–42.

Friesen, T.L., Ali, S., Kianian, S., Francl, L.J. and Rasmussen, J.B. (2003) Role of host sensitivity to Ptr ToxA in development of tan spot of wheat. *Phytopathology*, **93**, 397–401.

Friesen, T.L., Stukenbrock, E.H., Liu, Z., Meinhardt, S., Ling, H., Faris, J.D., Rasmussen, J.B., Solomon, P.S., McDonald, B.A. and Oliver, R.P. (2006) Emergence of a new disease as a result of interspecific virulence gene transfer. *Nat. Genet.* **38**, 953–956.

Friesen, T.L., Meinhardt, S.W. and Faris, J.D. (2007) The *Stagonospora nodorum*–wheat pathosystem involves multiple proteinaceous host-selective toxins and corresponding host sensitivity genes that interact in an inverse gene-for-gene manner. *Plant J.* **51**, 681–692.

Friesen, T.L., Faris, J.D., Solomon, P.S. and Oliver, R.P. (2008) Host-specific toxins: effectors of necrotrophic pathogenicity. *Cell. Microbiol.* **10**, 1421–1428.

Gessner, M. (2005) Ergosterol as a measure of fungal biomass. In: *Methods to Study Litter Decomposition* (Graça, M.A.S., Bärlocher, F. and Gessner, M.O., eds), pp. 189–195. Dordrecht, the Netherlands: Springer.

Goodwin, S.B., Ben M'Barek, S., Dhillon, B., Wittenberg, A.H.J., Crane, C.F., Hane, J.K., Foster, A.J., van der Lee, T.A.J., Grimwood, J., Aerts, A., Antoniw, J., Bailey, A., Bluhm, B., Bowler, J., Bristow, J., van der Burgt, A., Canto-Canché, B., Chunrchill, A.C.L., Conde-Ferràez, L., Cools, H.J., Coutinho, P.M., Csukai, M., Dehal, P., de Wit, P., Donzelli, B., van de Geest, H.C., van Ham, R.C.H.J., Hammond-Kosack, K.E., Henrissat, B., Kilian, A., Kobayashi, A.K., Koopmann, E., Kourmpetis, Y., Kuzniar, A., Lindquist, E., Lombard, V., Maliepaard, C., Martins, N., Mehrabi, R., Nap, J.P.H., Ponomarenko, A., Rudd, J.J., Salamov, A., Schmutz, J., Schouten, H.J., Shapiro, H., Stergiopoulos, I., Torriani, S.F.F., Tu, H., de Vries, R.P., Waalwijk, C., Ware, S.B., Wiebenga, A., Zwiers, L.H., Oliver, R.P., Grigoriev, I.V. and Kema, G.H.J. (2011) Finished genome of the fungal wheat pathogen *Mycosphaerella graminicola* reveals dispensome structure, chromosome plasticity, and stealth pathogenesis. *PLoS Genet.* **7**, e1002070.

Guldener, U., Seong, K.Y., Boddu, J., Cho, S., Trail, F., Xu, J.R., Adam, G., Mewes, H.W., Muehlbauer, G.J. and Kistler, H.C. (2006) Development of a *Fusarium graminearum* Affymetrix GeneChip for profiling fungal gene expression in vitro and in planta. *Fungal Genet. Biol.* **43**, 316–325.

Hahn, M. and Mendgen, K. (2001) Signal and nutrient exchange at biotrophic plant–fungus interfaces. *Curr. Opin. Plant Biol.* **4**, 322–327.

Hane, J.K., Lowe, R.G., Solomon, P.S., Tan, K.C., Schoch, C.L., Spatafora, J.W., Crous, P.W., Kodira, C., Birren, B.W., Galagan, J.E., Torriani, S.F., McDonald, B.A. and Oliver, R.P. (2007) Dothideomycete plant interactions illuminated by genome sequencing and EST analysis of the wheat pathogen *Stagonospora nodorum*. *Plant Cell*, **19**, 3347–3368.

Hane, J.K., Williams, A. and Oliver, R.P. (2011) Genomic and comparative analysis of the class Dothideomycetes. In: *The Mycota* (Poggeler, S. and Wostemeyer, J., eds), pp. 205–226. Berlin: Springer-Verlag.

Howard, K., Foster, S.G., Cooley, R.N. and Caten, C.E. (1999) Disruption, replacement, and cosuppression of nitrate assimilation genes in *Stagonospora nodorum*. *Fungal Genet. Biol.* **26**, 152–162.

Irizarry, R.A., Hobbs, B., Collin, F., Beazer-Barclay, Y.D., Antonellis, K.J., Scherf, U. and Speed, T.P. (2003) Exploration, normalization, and summaries of high density oligonucleotide array probe level data. *Biostat*, **4**, 249–264.

Jung, H.W., Tschaplinski, T.J., Wang, L., Glazebrook, J. and Greenberg, J. (2009) Priming in systemic plant immunity. *Science*, **324**, 89–91.

Kamper, J., Kahmann, R., Bolker, M., Ma, L.J., Brefort, T., Saville, B.J., Banuett, F., Kronstad, J.W., Gold, S.E., Muller, O., Perlin, M.H., Wosten, H.A.B., de Vries, R., Ruiz-Herrera, J., Reynaga-Pena, C.G., Snetselaar, K., McCann, M., Perez-Martin, J., Feldbrugge, M., Basse, C.W., Steinberg, G., Ibeas, J.I., Holloman, W., Guzman, P., Farman, M., Stajich, J.E., Sentandreu, R., Gonzalez-Prieto, J.M., Kennell, J.C., Molina, L., Schirawski, J., Mendoza-Mendoza, A., Greilinger, D., Munch, K., Rossel, N., Scherer, M., Vranes, M., Ladendorf, O., Vincon, V., Fuchs, U., Sandrock, B., Meng, S., Ho, E.C.H., Cahill, M.J., Boyce, K.J., Klose, J., Klosterman, S.J., Deelstra, H.J., Ortiz-Castellanos, L., Li, W.X., Sanchez-Alonso, P., Schreier, P.H., hauser-Hahn, I., Vaupel, M., Koopmann, E., Friedrich, G., Voss, H., Schluter, T., Margolis, J., Platt, D., Swimmer, C., Gnirke, A., Chen, F., Vysotskaia, V., Mannhaupt, G., Guldener, U., Munsterkotter, M., Haase, D., Oesterheld, M., Mewes, H.W., Mauceli, E.W., DeCaprio, D., Wade, C.M., Butler, J., Young, S., Affe, D.B.J., Calvo, S., Nusbaum, C., Galagan, J. and Birre, B.W. (2006) Insights from the genome of the biotrophic fungal plant pathogen *Ustilago maydis*. *Nature*, **444**, 97–101.

Keon, J., Rudd, J.J., Antoniw, J., Skinner, W., Hargreaves, J. and Hammond-Kosack, K. (2005) Metabolic and stress adaptation by *Mycosphaerella graminicola* during sporulation in its host revealed through microarray transcription profiling. *Mol. Plant Pathol.* **6**, 527–540.

Knight, S.C., Anthony, V.M., Brady, A.M., Greenland, A.J., Heaney, S.P., Murray, D.C., Powell, K.A., Schulz, M.A., Spinks, C.A., Worthington, P.A. and Youle, D. (1997) Rationale and perspectives on the development of fungicides. *Annu. Rev. Phytopathol.* **35**, 349–372.

Langfelder, K., Streibel, M., Jahn, B., Haase, G. and Brakhage, A.A. (2003) Biosynthesis of fungal melanins and their importance for human pathogenic fungi. *Fungal Genet. Biol.* **38**, 143–158.

Liu, Z., Friesen, T.L., Ling, H., Meinhardt, S.W., Oliver, R.P., Rasmussen, J.B. and Faris, J.D. (2006) The Tsn1–ToxA interaction in the wheat–*Stagonospora nodorum* pathosystem parallels that of the wheat–tan spot system. *Genome*, **49**, 1265–1273.

Liu, Z., Faris, J.D., Oliver, R.P., Tan, K.C., Solomon, P.S., McDonald, M.C., McDonald, B.A., Nunez, A., Lu, S., Rasmussen, J.B. and Friesen, T.L. (2009) SnTox3 acts in effector triggered susceptibility to induce disease on wheat carrying the Snn3 gene. *PLoS Pathog.* **5**, e1000581.

Manuela, A. (2009) ATP and ergosterol as indicators of fungal biomass during leaf decomposition in streams: a comparative study. *Int. Rev. Hydrobiol.* **94**, 3–15.

Marthey, S., Aguileta, G., Rodolphe, F., Gendrault, A., Giraud, T., Fournier, E., Lopez-Villavicencio, M., Gautier, A., lebrun, M.H. and Chiapello, H. (2008) FUNYBASE: a FUNgal phYlogenomic dataBASE. *BMC Bioinformatics*, **9**, 456.

Meinhardt, S.W., Cheng, W., Kwon, C.Y., Donohue, C.M. and Rasmussen, J.B. (2002) Role of the arginyl–glycyl–aspartic motif in the action of Ptr ToxA produced by *Pyrenophora tritici-repentis*. *Plant Physiol.* **130**, 1545–1551.

Murray, G.M. and Brennan, J.P. (2009) Estimating disease losses to the Australian wheat industry. *Australas. Plant Pathol.* **38**, 558–570.

Oliver, R.P. (2008) Plant breeding for disease resistance in the age of effectors. *Phytoparasitica*, **37**, 1–5.

Oliver, R.P. and Ipcho, S.V.S. (2004) Arabidopsis pathology breathes new life into the necrotrophs-vs.-biotrophs classification of fungal pathogens. *Mol. Plant Pathol.* **5**, 347–352.

Oliver, R.P. and Solomon, P.S. (2004) Does the oxidative stress used by plants for defence provide a source of nutrients for pathogenic fungi? *Trends Plant Sci.* **9**, 472–473.

Oliver, R.P. and Solomon, P.S. (2010) New developments in pathogenicity and virulence of necrotrophs. *Curr. Opin. Plant Biol.* **13**, 415–419.

Persson, B.L., Berhe, A., Fristedt, U., Martinez, P., Pattison, J., Petersson, J. and Weinander, R. (1998) Phosphate permeases of *Saccharomyces cerevisiae*. *Biochim. Biophys. Acta Bioenerg.* **1365**, 23–30.

Rouxel, T., Grandaubert, J., Hane, J., Hoede, C., van de Wouw, A., Couloux, A., Dominguez, V., Anthouard, V., Bally, P., Bourras, S., Cozijnsen, A., Ciuffetti, L., Dimaghani, A., Duret, L., Fudal, I., Goodwin, S., Gout, L., Glaser, N., Kema, G., Lapalu, N., Lawrence, C., May, K., Meyer, M., Ollivier, B., Poulain, J., Turgeon, G., Tyler, B.M., Vincent, D., Weissenbach, J., Amselem, J., Balesdent, M.-H., Howlett, B.J., Oliver, R., Quesneville, H. and Wincker, P. (2011) The compartmentalized genome of *Leptosphaeria maculans*: diversification of effectors within genomic regions affected by Repeat Induced Point mutations. *Nat. Commun.* **2**, art. 202.

Schoch, C.L., Shoemaker, R.A., Seifert, K.A., Hambleton, S., Spatafora, J.W. and Crous, P.W. (2006) A multigene phylogeny of the Dothideomycetes using four nuclear loci. *Mycologia*, **98**, 1043–1054.

Schoch, C.L., Crous, P.W., Groenewald, J.Z., Boehm, E.W., Burgess, T.I., de Gruyter, J., de Hoog, G.S., Dixon, L.J., Grube, M., Gueidan, C., Harada, Y., Hatakeyama, S., Hirayama, K., Hosoya, T., Huhndorf, S.M., Hyde, K.D., Jones, E.B., Kohlmeyer, J., Kruys, A., Li, Y.M., Lucking, R., Lumbsch, H.T., Marvanova, L., Mbatchou, J.S., McVay, A.H., Miller, A.N., Mugambi, G.K., Muggia, L., Nelson, M.P., Nelson, P., Owensby, C.A., Phillips, A.J., Phongpaichit, S., Pointing, S.B., Pujade-Renaud, V., Raja, H.A., Plata, E.R., Robbertse, B., Ruibal, C., Sakayaroj, J., Sano, T., Selbmann, L., Shearer, C.A., Shirouzu, T., Slippers, B., Suetrong, S., Tanaka, K., Volkmann-Kohlmeyer, B., Wingfield, M.J., Wood, A.R., Woudenberg, J.H., Yonezawa, H., Zhang, Y. and Spatafora, J.W. (2009) A class-wide phylogenetic assessment of Dothideomycetes. *Stud. Mycol.* **64**, 1–15.

da Silva Ferreira, M.E., Savoldi, M., Sueli Bonato, P., Goldman, M.H.S. and Goldman, G.H. (2006) Fungal metabolic model for tyrosinemia type 3: molecular characterization of a gene encoding a 4-hydroxy-phenyl pyruvate dioxygenase from *Aspergillus nidulans*. *Eukaryot. Cell*, **5**, 1441–1445.

Solomon, P.S. and Oliver, R.P. (2002) Evidence that γ-aminobutyric acid is a major nitrogen source during *Cladosporium fulvum* infection of tomato. *Planta*, **214**, 414–420.

Solomon, P.S., Tan, K.-C. and Oliver, R.P. (2003a) The nutrient supply of pathogenic fungi; a fertile field for study. *Mol. Plant Pathol.* **4**, 203–210.

Solomon, P.S., Thomas, S.W., Spanu, P. and Oliver, R.P. (2003b) The utilisation of di/tripeptides by *Stagonospora nodorum* is dispensable for wheat infection. *Physiol. Mol. Plant Pathol.* **63**, 191–199.

Solomon, P.S., Lee, R.C., Wilson, T.J.G. and Oliver, R.P. (2004a) Pathogenicity of *Stagonospora nodorum* requires malate synthase. *Mol. Microbiol.* **53**, 1065–1073.

Solomon, P.S., Tan, K.C., Sanchez, P., Cooper, R.M. and Oliver, R.P. (2004b) The disruption of a Gα subunit sheds new light on the pathogenicity of *Stagonospora nodorum* on wheat. *Mol. Plant–Microbe Interact.* **17**, 456–466.

Solomon, P.S., Jörgens, C.I. and Oliver, R.P. (2006a) δ-Aminolaevulinic acid synthesis is required for virulence of the wheat pathogen *Stagonospora nodorum*. *Microbiology*, **152**, 1533–1538.

Solomon, P.S., Lowe, R.G.T., Tan, K.C., Waters, O.D.C. and Oliver, R.P. (2006b) *Stagonospora nodorum*: cause of stagonospora nodorum blotch of wheat. *Mol. Plant Pathol.* **7**, 147–156.

Solomon, P.S., Rybak, K., Trengove, R.D. and Oliver, R.P. (2006c) Investigating the role of calcium/calmodulin-dependent protein kinases in *Stagonospora nodorum*. *Mol. Microbiol.* **62**, 367–381.

Solomon, P.S., Wilson, T.J.G., Rybak, K., Parker, K., Lowe, R.G.T. and Oliver, R.P. (2006d) Structural characterisation of the interaction between *Triticum aestivum* and the dothideomycete pathogen *Stagonospora nodorum*. *Eur. J. Plant Pathol.* **114**, 275–282.

Solomon, P.S., Ipcho, S.V.S., Hane, J.K., Tan, K.C. and Oliver, R.P. (2008) A quantitative PCR approach to determine gene copy number. *Fungal Genet. Rep.* **55**, 5–8.

Spry, C., Kirk, K. and Saliba, K.J. (2008) Coenzyme A biosynthesis: an antimicrobial drug target. *FEMS Microbiol. Rev.* **32**, 56–106.

Stephens, A.E., Gardiner, D.M., White, R.G., Munn, A.L. and Manners, J.M. (2008) Phases of infection and gene expression of *Fusarium graminearum* during crown rot disease of wheat. *Mol. Plant–Microbe Interact.* **21**, 1571–1581.

Tan, K.C., Ipcho, S.V.S., Trengove, R.D., Oliver, R.P. and Solomon, P.S. (2009) Assessing the impact of transcriptomics, proteomics and metabolomics on fungal phytopathology. *Mol. Plant Pathol.* **10**, 703–715.

Tavernier, V., Cadiou, S., Pageau, K., Laugé, R., Reisdorf-Cren, M., Langin, T. and Masclaux-Daubresse, C. (2007) The plant nitrogen mobilization promoted by *Colletotrichum lindemuthianum* in *Phaseolus* leaves depends on fungus pathogenicity. *J. Exp. Bot.* **58**, 3351–3360.

Versaw, W.K. (1995) A phosphate-repressible, high-affinity phosphate permease is encoded by the pho-5+ gene of *Neurospora crassa*. *Gene*, **153**, 135–139.

Wykoff, D.D. and O'Shea, E.K. (2001) Phosphate transport and sensing in *Saccharomyces cerevisiae*. *Genetics*, **159**, 1491–1499.

SUPPORTING INFORMATION

Additional Supporting Information may be found in the online version of this article:

Fig. S1 The reliability of the microarray data was tested by analysing the expression trend of three genes using quantitative reverse transcription-polymerase chain reaction (qRT-PCR). The expression trend was found to be the same by both techniques and hence showed that the microarray data were reliable. *N.D., the expression of this transcript was not detected *in vitro* by either technique.

Fig. S2 Box plots illustrating the range of gene expression level from each array after normalization. The lower and upper ends of the box represent the 25th and 75th percentiles, respectively, and the whiskers show the extreme values of the distribution. The white line within the box represents the 50th percentile or median, and the red diamond shows the mean value of the distribution. The relative uniformity of the box plots shows that the arrays were properly normalized and that there were no outliers.

Fig. S3 Gene structure and primer positions used to ablate SNOG_08736.

Fig. S4 Structure of knockout construct and polymerase chain reaction (PCR) analysis of knocked out strains.

Table S1 The average intensity of genes from SN79-1087 that did not map to SN15 genes. The intensities from the 112 genes were used to calculate a background reading on the arrays.

Table S2 Primer sequences used to analyse SNOG_08736.

Please note: Wiley-Blackwell are not responsible for the content or functionality of any supporting materials supplied by the authors. Any queries (other than missing material) should be directed to the corresponding author for the article.

